Collaborative Direction-of-Arrival Estimation Exploiting One-Bit Cross-Correlations

Yimin D. Zhang [1] and Ashley Prater-Bennette [2]

[1] Department of Electrical and Computer Engineering, Temple University, Philadelphia, PA 19122, USA
[2] Information Directorate, Air Force Research Laboratory, Rome, NY 13441, USA

***Abstract*—In this paper, we consider a collaborative direction-of-arrival (DOA) estimation problem in which multiple quasi-collocated subarrays are employed. Our objective is to effectively utilize the full potential offered by the distributed array with minimum communication traffic between the subarrays and the processing center. In the proposed scheme, each subarray computes the self-subarray covariance matrix with the full precision. Each subarray then sends the estimated covariance matrix together with the one-bit version of the raw data to the processing center. The processing center computes the cross-subarray covariance matrices between different subarrays based on the one-bit data, which, together with the self-subarray covariance matrices which are computed and reported by the subarrays, are used to estimate the source DOAs. The combined exploitation of the full-precision self-subarray covariance matrices and the low-precision cross-subarray covariance matrices ensures full degrees of freedom offered by the array with only slight performance loss compared with the case where all covariance matrices are provided with full precision.**

Keywords: Direction-of-arrival estimation, collaborative network, structured matrix completion, degree of freedom.

I. Introduction

Collaborative sensing and network communication systems using distributed sensor array platforms are becoming increasingly attractive in various civil and military applications [1–6]. In this work, we consider a collaborative platform where multiple subarrays are employed to estimate source directions-of-arrival (DOAs). These subarrays are considered quasi-collocated, i.e., they are closely distributed such that the difference in the observed impinging angles due to the subarray locations is negligible. Unmanned aerial vehicles (UAVs), each equipped with an array, are a good example for such a platform. It is note that, in each subarray, the number of sensors may or may not be identical, and the array sensors may be spaced uniformly, sparsely with the same configuration, or sparsely with different configurations.

In such a distributed array platform, DOA estimation can be achieved either coherently or non-coherently. In coherent DOA estimation problems, all the array data observed at each subarray are transmitted to a processing center. Assuming complete subarray synchronization and accurate position information of each subarray, such subarrays form a big array with sparsely located subarray sensors. When the sensor positions are accurately calibrated in each subarray with respect to their own reference sensors whereas the relatively positions of the subarrays are not precisely known, the formed array is often referred to as partly calibrated array and the DOA estimation problem is addressed in, e.g., [7].

Implementing coherent processing for the data observed at different subarrays, however, requires several demanding conditions. One of the strict requirements is to synchronously sample and transfer raw data to the processing center. This requirement, among others, generates a high volume of data traffic between the subarrays and the processing center. To avoid such communication overhead, a much simpler alternative strategy is to process the subarray data non-coherently [8, 9]. In this case, each subarray locally computes its covariance matrix, which is then forwarded to the processing center. Compared with the raw data, transferring only the covariance matrices yields significant reduction in the communication overhead. A clear disadvantage of non-coherent processing, however, is the substantial loss of the available degrees of freedom and the DOA estimation performance.

In this paper, we consider a generalized strategy in which, in addition to the full-precision self-subarray covariance matrices which are computed at each subarray and forwarded to the processing center, the one-bit version of the raw data is also sent to the processing center. Compared to the full-precision raw data, one-bit data greatly lower the communication overhead. The covariance matrix obtained from one-bit quantized signals is related to the full-precision covariance matrix with a arcsin relationship [10]. Based on this finding, one-bit data-based processing is found attractive in many array and multiple-input multiple-output (MIMO) processing problems, including channel estimation and DOA estimation [11–19].

This paper will formulate the signal model of the proposed collaborative DOA estimation scheme and describe the signal processing procedures including the local processing at each subarray and the centralized processing at the processing center. The performance of the proposed scheme is numerically examined and compared to different situations where

The work of Y. D. Zhang was supported in part by the 2021 Air Force Research Laboratory Summer Faculty Fellowship Program. Any opinions, findings, conclusions or recommendations expressed in this material are those of the authors and do not necessarily reflect the view of the United States Air Force.

the cross-subarray covariance matrices are estimated with full-precision data or are totally unavailable. It is learned that the proposed scheme maintains the full degrees of freedom offered by the coherent DOA estimation scheme with mild performance degradation compared to the case where the covariance matrices are computed with a full precision. It significant outperforms the case when cross-subarray covariance matrices are unavailable.

Notations: We use lower-case (upper-case) bold characters to denote vectors (matrices). In particular, $\mathbf{I}_N$ denotes the $N \times N$ identity matrix. $(.)^{\mathrm{T}}$ and $(.)^{\mathrm{H}}$ respectively represent the transpose and conjugate transpose of a matrix or a vector. Furthermore, $[\mathbf{A}]_{u,v}$ denotes the (u,v)th element of matrix $\mathbf{A}$, and $\mathbb{E}[\cdot]$ is the statistical expectation operator. $\mathcal{Q}(\cdot)$ denotes the one-bit quantization operation, and $\mathrm{Re}(\cdot)$ and $\mathrm{Im}(\cdot)$ respectively denote the real and imaginary parts of a complex entry.

II. System Model

Consider a collaborative array platform consisting of K quasi-collocated subarrays. For simplicity but without loss of generality, it is assumed that all subarrays are M-element uniform linear arrays with interelement spacing of $d = \lambda/2$ with λ denoting the signal wavelength. Denoting $p_{k,1}d$ as the position of the first sensor at the kth subarray, the locations of the M sensors in the kth subarray are denoted by the following position set:

$$\begin{aligned}\mathbb{S}_k &= \{p_{k,1}d, p_{k,2}d, \ldots, p_{k,M}d\} \\ &= \{p_{k,1}d, (p_{k,1}+1)d, \ldots, (p_{k,1}+M-1)d\}\end{aligned} \tag{1}$$

for $k = 1, \ldots, K$. In this paper, it is assumed that the subarrays are fully synchronized, and the subarray locations are precisely known. In addition, the values of $p_{k,1}$ are assumed to be integers, i.e., all subarray sensors are an aligned with a half-wavelength grid. As such the array aperture is expressed as $P = p_{K,1} + M - 1$.

Consider L uncorrelated far-field narrow-band signals impinging on all K subarrays from distinct angles $\{\theta_1, \cdots, \theta_L\}$. The baseband signal vector received at the kth sparse subarray is expressed as:

$$\mathbf{x}_k(t) = \sum_{l=1}^{L} \mathbf{a}_k(\theta_l) s_l(t) + \mathbf{n}_k(t) = \mathbf{A}_k \mathbf{s}(t) + \mathbf{n}_k(t), \tag{2}$$

where $s_l(t)$ denotes the uncorrelated signal waveform impinging from direction θ_l, $\mathbf{s}(t) = [s_1(t), \cdots, s_L(t)]^{\mathrm{T}}$, and

$$\mathbf{a}_k(\theta) = [e^{-jp_{k,1}\pi\sin(\theta)}, e^{-jp_{k,2}\pi\sin(\theta)}, \ldots e^{-jp_{k,M}\pi\sin(\theta)}]^{\mathrm{T}} \tag{3}$$

is the steering vector of the kth subarray corresponding to a signal impinging from angle θ. In addition, $\mathbf{A}_k = [\mathbf{a}_k(\theta_1), \mathbf{a}_k(\theta_2), \ldots, \mathbf{a}_k(\theta_L)]$ is referred to as the manifold matrix of the kth subarray, and $\mathbf{n}_k(t) \sim \mathcal{CN}(\mathbf{0}, \sigma^2_{\mathrm{n},k}\mathbf{I}_M)$ represents the additive circularly complex white Gaussian noise vector observed at the kth subarray.

III. Estimation of Covariance Matrices and Signal DOAs

In this section, we first address the processing procedures at the local subarray and at the processing center to compute the covariance matrix. The DOA estimation approach is then considered.

A. Local Processing at Subarrays

The self-subarray covariance matrix of the received data for the kth subarray is given as:

$$\begin{aligned}\mathbf{R}_k &= \mathbb{E}[\mathbf{x}_k(t)\mathbf{x}_k^{\mathrm{H}}(t)] = \mathbf{A}_k \mathbf{R}_{\mathbf{ss}} \mathbf{A}_k^{\mathrm{H}} + \sigma^2_{\mathrm{n},k}\mathbf{I}_M \\ &= \sum_{l=1}^{L} \sigma_l^2 \mathbf{a}_k(\theta_l)\mathbf{a}_k^{\mathrm{H}}(\theta_l) + \sigma^2_{\mathrm{n},k}\mathbf{I}_M,\end{aligned} \tag{4}$$

where $\mathbf{R}_{\mathbf{ss}} = \mathbb{E}[\mathbf{s}(t)\mathbf{s}^{\mathrm{H}}(t)] = \mathrm{diag}([\sigma_1^2, \sigma_2^2, \cdots, \sigma_L^2])$ is the source covariance matrix with σ_l^2 denoting the power of the lth source, $l = 1, \ldots, L$.

In practice, the self-subarray covariance matrix of the kth subarray is estimated using the T available data samples, expressed as,

$$\hat{\mathbf{R}}_k = \frac{1}{T}\sum_{t=1}^{T} \mathbf{x}_k(t)\mathbf{x}_k^{\mathrm{H}}(t). \tag{5}$$

It is note that, for a uniform linear subarray, $\hat{\mathbf{R}}_k$ is Hermitian and Toeplitz. As such, the entire matrix can be determined from the first column [20]. In other words, only the first column needs to be sent to the process center.

In addition to the self-subarray covariance matrix, the kth subarray performs complex one-bit quantization of the received data. The real and imaginary parts of the complex signal vector $\mathbf{x}_k(t)$ are respectively quantized to form a one-bit version of this signal vector as

$$\mathbf{y}_k(t) = \frac{1}{\sqrt{2}}\left\{\mathcal{Q}[\mathrm{Re}(\mathbf{x}_k(t))] + j\mathcal{Q}[\mathrm{Im}(\mathbf{x}_k(t))]\right\}. \tag{6}$$

The resulting $\mathbf{y}_k(t)$ is transferred to the processing center, possibly with a decimated rate of $\kappa \geq 1$ so that only $T_0 = T/\kappa$ samples are transferred.

B. Centralized Processing at the Processing Center

The cross-subarray covariance matrix between the received data at the k_1th and k_2th subarrays is given as:

$$\begin{aligned}\mathbf{R}_{k_1k_2} &= \mathbb{E}[\mathbf{x}_{k_1}(t)\mathbf{x}_{k_2}^{\mathrm{H}}(t)] \\ &= \mathbf{A}_{k_1}\mathbf{S}\mathbf{A}_{k_2}^{\mathrm{H}} = \sum_{l=1}^{L} \sigma_l^2 \mathbf{a}_{k_1}(\theta_l)\mathbf{a}_{k_2}^{\mathrm{H}}(\theta_l),\end{aligned} \tag{7}$$

for $k_1, k_2 = 1, \ldots, K$, $k_1 \neq k_2$.

When the full-precision and complete T-sample data are available at the processing center, the above cross-subarray covariance matrix is estimated as

$$\hat{\mathbf{R}}_{k_1k_2} = \frac{1}{T}\sum_{t=1}^{T} \mathbf{x}_{k_1}(t)\mathbf{x}_{k_2}^{\mathrm{H}}(t). \tag{8}$$

On the other hand, when only T_0 samples of one-bit data samples are provided, the one-bit cross-subarray covariance matrix between the k_1th and k_2th subarrays is estimated as,

$$\hat{\mathbf{R}}_{k_1k_2}^{[1\mathrm{B}]} = \frac{1}{T_0}\sum_{t=1}^{T_0}\mathbf{y}_{k_1}(t)\mathbf{y}_{k_2}^{\mathrm{H}}(t), \tag{9}$$

where superscript [1B] is added to emphasize it being a one-bit estimate.

In general, the correlation $R_Z(\tau)$ between $z(t)$ and $z(t+\tau)$ is related to the one-bit result $R_Z^{[1\mathrm{B}]}(\tau)$ as [10, 21]

$$R_z^{[1\mathrm{B}]}(\tau) = \frac{2}{\pi}\sin^{-1}\left(\frac{R_z(\tau)}{R_z(0)}\right). \tag{10}$$

Note here that the one-bit auto-correlation function is normalized because the one-bit quantization result does not carry information of the signal magnitude. Similarly, the cross-covariance between $z_1(t)$ and $z_2(t+\tau)$ can be obtained

$$R_{z_1z_2}^{[1\mathrm{B}]}(\tau) = \frac{2}{\pi}\sin^{-1}\left(\frac{R_{z_1z_2}(\tau)}{\sqrt{R_{z_1}(0)R_{z_2}(0)}}\right). \tag{11}$$

As a result, the cross-subarray covariance matrix $\hat{\mathbf{R}}_{k_1k_2}$ is obtained from $\hat{\mathbf{R}}_{k_1k_2}^{[1\mathrm{B}]}$ as

$$\hat{\mathbf{R}}_{k_1k_2} = \mathbf{G}_1^{1/2}\bar{\mathbf{R}}_{k_1k_2}\mathbf{G}_2^{1/2}, \tag{12}$$

where $\mathbf{G}_k$ is a diagonal matrix with $[\mathbf{G}_k]_{m,m} = [\hat{\mathbf{R}}_k]_{m,m}$, $m = 1, \cdots, M$, and

$$\bar{\mathbf{R}}_{k_1k_2} = \sin\left(\frac{\pi}{2}\mathrm{Re}[\hat{\mathbf{R}}_{k_1k_2}^{[1\mathrm{B}]}]\right) + j\sin\left(\frac{\pi}{2}\mathrm{Im}[\hat{\mathbf{R}}_{k_1k_2}^{[1\mathrm{B}]}]\right). \tag{13}$$

Combining the self- and cross-subarray covariance matrices, we form the full covariance matrix of all KM sensors at the processing center as:

$$\hat{\mathbf{R}} = \begin{bmatrix} \hat{\mathbf{R}}_1 & \mathbf{0} & \hat{\mathbf{R}}_{1,2} & \mathbf{0} & \cdots & \mathbf{0} & \hat{\mathbf{R}}_{1,K} \\ \hat{\mathbf{R}}_{2,1} & \mathbf{0} & \hat{\mathbf{R}}_2 & \mathbf{0} & \cdots & \mathbf{0} & \hat{\mathbf{R}}_{2,3} \\ \vdots & \vdots & \vdots & \vdots & \ddots & \vdots & \vdots \\ \hat{\mathbf{R}}_{K,1} & \mathbf{0} & \hat{\mathbf{R}}_{K,2} & \mathbf{0} & \cdots & \mathbf{0} & \hat{\mathbf{R}}_K \end{bmatrix}, \tag{14}$$

where $\mathbf{0}$ denotes missing sensor positions when the inter-subarray spacing is larger than half-wavelength. DOA estimation using the full covariance matrix is described in Section III-C.

An example of the resulting covariance matrix is illustrated in Fig. 1 for an example of $K = 3$ and $M = 4$. The positions of the respective first sensors of the three subarrays are given as $[0, 5, 11]d$. Note again that the self-subarray covariance matrices, illustrated in blue color circles, have the full estimation accuracy, whereas the cross-subarray covariance matrices, depicted in green color circles, have reduced estimation accuracy due to one-bit quantization and possibly lower number of data samples. The circles showing with magenta dashed lines depict missing positions.

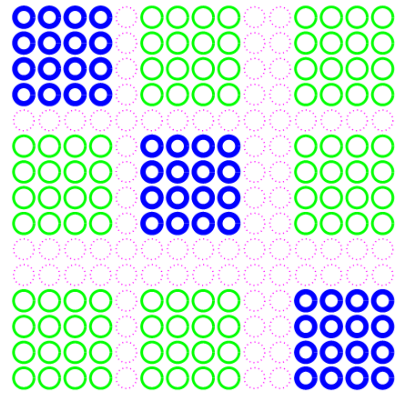

Fig. 1: Example of full covariance matrix ($K = 3$ and $M = 4$).

C. DOA Estimation Methods

When all the self- and cross-subarray covariance matrices are available at the processing center in full precision, DOA estimation can be carried out using conventional subspace-based method, such as the popularly used MUSIC [22]. When the cross-subarray covariance matrices have a reduced precision, MUSIC remains applicable. On the other hand, when cross-subarray covariance matrices are unavailable, the total covariance matrix is incomplete. In this case, MUSIC works robustly only when considering a single subarray or the averaged covariance matrix of the subarrays, thus only handles up to $M - 1$ sources. Directly applying MUSIC to the total covariance matrix without cross-correlation matrices generally does not render meaningful DOA estimation results.

The Toeplitz and Hermitian structure of the full covariance matrix can be used to fill in missing entries. That is, if a single or multiple covariance entries are available for a specific lag, this value or the averaged value of these entries can be used to fill in missing entries corresponding to the same lag. When there are still missing entries, we can fully utilize matrix completion utilizing the Toeplitz and Hermitian structure to improve the full covariance matrix [20, 23–26]. Note that these methods work well even a substantial portion of the total covariance matrices is not filled in the previous stage due to, for example, sparse subarray designs or large inter-subarray spacing. After the full covariance matrix is reconstructed, the MUSIC algorithm can be applied to perform DOA estimation in a gridless manner.

IV. Numerical Results

We consider a simple example using the distributed array configuration depicted in Fig. 1. A varying number of L uncorrelated sources are assumed to be uniformly distributed between $-50°$ and $50°$. We consider $T = 200$ data snapshots at each subarray and the input signal-to-noise ratio (SNR) is set to 0 dB.

A. Full-Precision Covariance Matrix Case

As the baseline for comparison, we first show the DOA estimation performance when both self- and cross-subarray

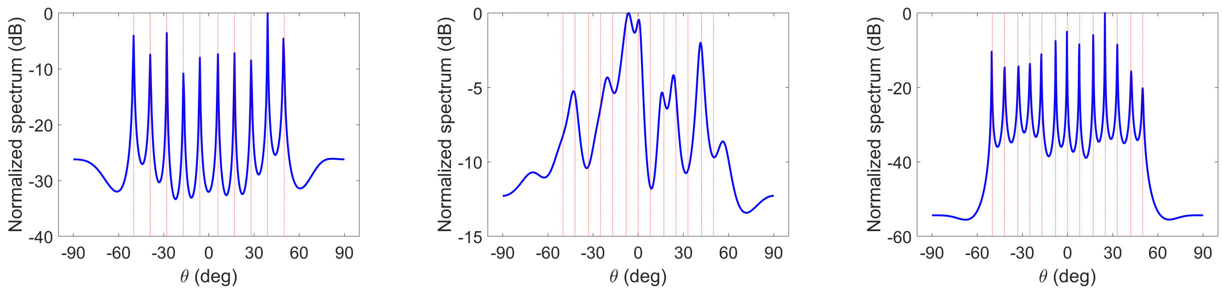

(a) No interpolation, 10 sources. (b) No interpolation, 13 sources. (c) With interpolation, 13 sources.

Fig. 2: MUSIC pseudo-spectra based on full-precision self- and cross-subarray covariance matrices.

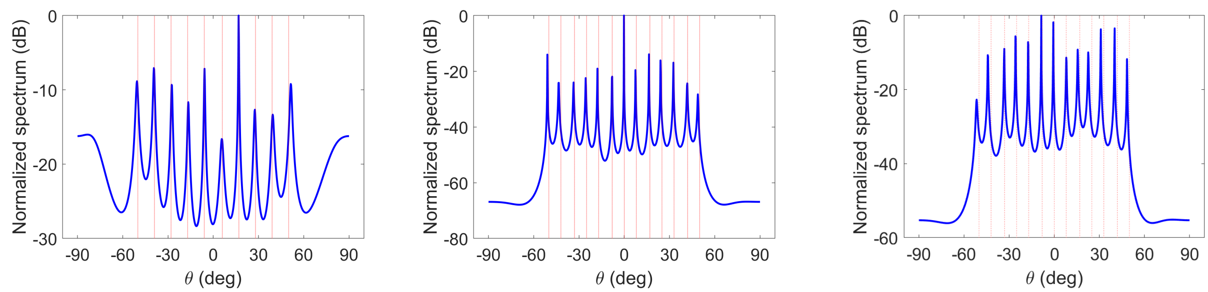

(a) No interpolation, 10 sources, $T_0 = 200$ (b) With interpolation, 13 sources, $T_0 = 200$ (c) With interpolation, 13 sources, $T_0 = 100$

Fig. 3: MUSIC pseudo-spectra where cross-subarray covariance matrices are computed from one-bit data.

covariance matrices are estimated using the full-precision data without quantization. Fig. 2(a) shows the MUSIC pseudo-spectrum when there are $L = 10$ sources, and no covariance matrix completion is performance. In this case, all sources are well resolved with a root mean-square error (RMSE) of $0.168°$. As there are 12 sensors in total, the distributed array resolves up to 11 sources. Therefore, when the number of sources is increased to 13, the MUSIC algorithm fail to resolve the sources, as depicted in Fig. 2(b). In Fig. 2(c), we present the results when matrix completion is performed. In this case, the dimension of the completed covariance matrix is 15×15, and all 13 sources are resolved with an RMSE of $0.368°$.

B. Exploiting Cross-Subarray Covariance Matrices Based on One-Bit Data

When one-bit data are forwarded from the subarrays to the processing center and used for cross-covariance matrix estimation, the distributed array still clearly resolve the signals as in the full-precision case, but the DOA estimation performance slightly degrades. We first consider the case where $T_0 = T = 200$. When matrix completion is not performed, similar to the case we considered in Fig. 2(a), the array does not recognize more than 11 sources. In Fig. 3(a), we show the results with the same 10 sources, and the RMSE is $0.580°$. On the other hand, when matrix completion is applied, Fig. 3(b) depicts the MUSIC pseudo-spectrum of 13 sources and the corresponding RMSE is $0.771°$.

Next, we reduce the number of one-bit data samples to $T_0 = 100$. As shown in Fig. 3(c), the distributed array still clearly detects all the 13 signals, but the estimation RMSE increases to $1.623°$.

V. Conclusion

This paper considers a new DOA estimation approach for distributed arrays which only requires the subarrays to send subarray covariance matrix and one-bit data to the processing center. It effectively utilizes the full potential offered by the distributed array whereas the network traffic is significantly reduced. The proposed DOA estimation approach ensures full degrees of freedom of the distributed array with only slight performance loss compared with the case where all covariance matrices are estimated using full-precision data.

VI. References

[1] A. Ryan, M. Zennaro, A. Howell, R. Sengupta, and J. Hedrick, “An overview of emerging results in cooperative UAV control,” in *Proc. IEEE Conf. Decision and Control*, May 2004, pp. 602—607.

[2] D. Cole, A. Goktogan, P. Thompson, and S. Sukkarieh, “Mapping and tracking,” *IEEE Robot. Autom. Mag.* , vol. 16, no. 2, pp. 22—34, June 2009.

[3] X. Li and Y. D. Zhang, “Multi-source cooperative communications using multiple small relay UAVs,” in *Proc.*

IEEE Globecom Workshop on Wireless Networking for Unmanned Aerial Vehicles, Miami, FL, Dec. 2010, pp. 1805–1810.

[4] B. K. Chalise, Y. D. Zhang, and M. G. Amin, "Multi-beam scheduling for unmanned aerial vehicle networks," in *Proc. IEEE/CIC Int. Conf. Commun. in China*, Xi'an, China, Aug. 2013, pp. 442–447.

[5] S. Hayat, E. Yanmaz, and R. Muzaffar, "Survey on unmanned aerial vehicle networks for civil applications: A communications viewpoint," *IEEE Commun. Surveys Tut.*, vol. 18, no. 4, pp. 2624–2661, 2016.

[6] E. Yanmaz, S. Yahyanejad, B. Rinner, H. Hellwagner, and C. Bettstetter, "Drone networks: Communications, coordination, and sensing," *Ad Hoc Networks*, vol. 68, pp. 1–15, Jan. 2018.

[7] M. Pesavento, A. B. Gershman, and K. M. Wong, "Direction finding in partly calibrated sensor arrays composed of multiple subarrays," *IEEE Trans. Signal Process.*, vol. 50, no. 9, pp. 2103–2115, Sept. 2002.

[8] P. Stoica, A. Nehorai, and T. Söderström, "Decentralized array processing using the MODE algorithm," *Circuits, Syst. Signal Process.*, vol. 14, no. 1, pp. 17—38, 1995.

[9] W. Suleiman, P. Parvazi, M. Pesavento, and A. M. Zoubir, "Non-coherent direction-of-arrival estimation using partly calibrated arrays," *IEEE Trans. Signal Process.*, vol. 66, no. 21, pp. 5776–5788, Nov. 2018.

[10] Y. Li, C. Tao, G. Seco-Granados, A. Mezghani, A. L. Swindlehurst, and L. Liu, "Channel estimation and performance analysis of one-bit massive MIMO systems," *IEEE Trans. Signal Process.*, vol. 65, no. 15, pp. 4075–4089, Aug. 2017.

[11] O. Bar-Shalom and A. J. Weiss, "DOA estimation using one-bit quantized measurements," *IEEE Trans. Aerosp. Electronic Syst.*, vol. 38, no. 3, pp. 868–884, July 2002.

[12] S. Jacobsson, G. Durisi, M. Coldrey, U. Gustavsson, and C. Studer, "One-bit massive MIMO: Channel estimation and high-order modulations," in *Proc. IEEE Int. Conf. Commun. Workshop (ICCW)*, London, U.K., June 2015, pp. 1304–1309.

[13] J. Mo and R. W. Heath, "Capacity analysis of one-bit quantized MIMO systems with transmitter channel state information," *IEEE Trans. Signal Process.*, vol. 63, no. 20, pp. 5498-5512, Oct. 2015.

[14] K. Yu, Y. D. Zhang, M. Bao, Y.-H. Hu, and Z. Wang, "DOA estimation from one-bit compressed array data via joint sparse representation," *IEEE Signal Process. Lett.*, vol. 23, no. 9, pp. 1279–1283, Sept. 2016.

[15] C. Liu and P. P. Vaidyanathan, "One-bit sparse array DOA estimation," in *Proc. IEEE Int. Conf. Acousti., Speech and Signal Process. (ICASSP)*, New Orleans, LA, pp. 3126–3130, 2017.

[16] P. Wang, J. Li, M. Pajovic, P. T. Boufounos, and P. V. Orlik, "On angular-domain channel estimation for one-bit massive MIMO systems with fixed and time-varying thresholds," in *Proc. Asilomar Conf. Signals, Systems, and Computers*, 2017, pp. 1056–1060.

[17] X. Huang and B. Liao, "One-bit MUSIC," *IEEE Signal Process. Lett.*, vol. 26, no. 7, pp. 961–965, July 2019.

[18] A. Ameri, A. Bose, J. Li, and M. Soltanalian, "One-bit radar processing with time-varying sampling thresholds," *IEEE Trans. Signal Process.*, vol. 67, no. 20, pp. 5297–5308, Oct. 2019.

[19] S. Sedighi, M. R. B. Shankar, M. Soltanalian, and B. Ottersten, "On the performance of one-bit DoA estimation via sparse linear arrays," https://arxiv.org/abs/2012.14051.

[20] C. Zhou, Y. Gu, X. Fan, Z. Shi, G. Mao, and Y. D. Zhang, "Direction-of-arrival estimation for coprime array via virtual array interpolation," *IEEE Trans. Signal Process.,* vol. 66, no. 22, pp. 5956–5971, Nov. 2018.

[21] J. H. Van Vleck and D. Middleton, "The spectrum of clipped noise," *Proc. IEEE*, vol. 54, no. 1, pp. 2—19, Jan. 1966.

[22] R. Schmidt, "Multiple emitter location and signal parameter estimation," *IEEE Trans. Antennas Propagat,*, vol. 34, no. 3, pp. 276–280, March 1986.

[23] H. Qiao and P. Pal, "Gridless line spectrum estimation and lowrank Toeplitz matrix compression using structured samplers: A regularization-free approach," *IEEE Trans. Signal Process.,* vol. 65, no. 9, pp. 2221–2236, May 2017.

[24] X. Wu, W.-P. Zhu, and J. Yan, "A Toeplitz covariance matrix reconstruction approach for direction-of-arrival estimation," *IEEE Trans. Veh. Technol.,* vol. 66, no. 9, pp. 8223–8237, Sep. 2017.

[25] C. Zhou, Y. Gu, Z. Shi, and Y. D. Zhang, "Off-grid direction-of-arrival estimation using coprime array interpolation," *IEEE Signal Process. Lett.*, vol. 25, no. 11, pp. 1710–1714, Nov. 2018.

[26] S. Liu, Z. Mao, Y. D. Zhang and Y. Huang, "Rank minimization-based Toeplitz reconstruction for DoA estimation using coprime array," *IEEE Commun. Lett.*, vol. 25, no. 7, pp. 2265–2269, July 2021.